Article:
Thompson, R, Austin, D, Wang, C et al. (2 more authors) (2021) Low-frequency plasma activation of nylon 6. Applied Surface Science, 544. 148929. ISSN 0169-4332

https://doi.org/10.1016/j.apsusc.2021.148929

Low-Frequency Plasma Activation of Nylon 6

Richard Thompson[a], David Austin[b], Chun Wang[c], Anne Neville[c], and Long Lin[a]*

[a]Department of Color Science, School of Chemistry, University of Leeds, Leeds, LS2 9JT, U.K.

[b]School of Chemical and Process Engineering, University of Leeds, Leeds, LS2 9JT, U.K.

[c]Institute of Functional Surfaces, School of Mechanical Engineering, University of Leeds, Leeds, LS2 9JT, U.K.

KEYWORDS: Plasma, plasma activation, surface modification, surface functionalization.

ABSTRACT: In the study reported in this paper, a series of reproducible conditions were employed to uniformly functionalize nylon 6 surfaces using a commercially available, low-frequency (40 kHz), low-pressure plasma system, utilizing oxygen plasma as a reactive gas. Initially, the plasma-treated samples were investigated using static contact angle measurements, showing a progressive increase in wettability with increasing plasma activation time between 10-40 s. Such an increase in wettability (and therefore increase in adhesive capabilities of the surfaces) was attributed to the creation of surface C-OH, C=O, and O=C-OH groups. These surface-chemical modifications were characterized using x-ray photoelectron spectroscopy (XPS) and static secondary ion mass spectrometry (SSIMS). Surface radical densities were also shown to increase following plasma activation, having been quantified using a radical scavenging method based on the molecule 2,2-diphenyl-1-picrylhydrazyl (DPPH). The samples were imaged and

analyzed using scanning electron microscopy (SEM) and atomic force microscopy (AFM), to confirm that there had been no detectable alteration to the surface roughness or morphology. Additionally, the "hydrophobic recovery" or "ageing" of the activated polymer samples, post-plasma treatment, was also investigated in terms of wettability and surface-chemistry, with the wettability of the sample surfaces decreasing over time due to a reduction in surface-oxygen concentration.

1. INTRODUCTION

The multi-billion dollar surface modification market is constantly increasing in size for polymer materials such as plastics and textiles, due to requirements to impart functional properties into these materials through environmentally benign methods. [1] Plasma technology proves to be an efficient, dry, substrate-independent, and green method for providing these surface treatments [2], avoiding the use of typically inefficient, traditional wet chemical methods. [3] Particularly in the textile industry, there is a significant drive by organizations such as the Zero Discharge of Hazardous Chemicals (ZDHC) towards producing resource efficient processes, completely eradicating the use of harsh chemicals. [4] In addition to being an environmentally friendly process, plasma also has the ability to produce products with a technical advantage, such as anti-microbial surfaces, super hydrophobic surfaces, and flame retardant surfaces. [3, 5-9] Worldwide demand for nylon 6 polymers have been increasing in recent years, due to the desirable properties of the material including high tensile strength, wrinkle and abrasion resistance, and high elasticity. [10] However, unmodified thermoplastics such as nylon 6 cannot meet all modern demands for different applications due to problems such as poor surface wettability, often leading to difficulties when applying functional coatings. [11] Therefore, understanding the fundamental interactions

between plasma gases and popular polymer materials such nylon 6 are crucially important to the development and optimization of plasma treatments for industrial processing. [12]

Plasma is considered to be the fourth aggregation state of matter, and can be identified as a partially ionized gas consisting of a mixture of reactive species including electrons, ions, radicals, neutral atoms, and charged particles. [13] When exposing polymer materials to non-polymerizing, reactive plasma gases such as oxygen, complex plasma-surface interactions on the nano-atomic scale enable material surfaces to be modified, without altering bulk material properties. [14] These modifications can be chemical, physical, or combinations of both, depending on the parameters selected. [12] Cold plasmas are of particular interest for the processing of heat-sensitive polymers (such as plastics and textiles), to prevent thermal decomposition. [15] Low-pressure plasma is a method of producing cold plasma, typically with a radiofrequency (RF) or microwave (MW) discharge. Using this process, materials can be treated with a constant gas flow, typically at pressures ranging from 0.2-0.5 mbar. [16] A major advantage of the low-pressure method is the ability to have full parameter control, including the ability to control gas flow in a reproducible manner, and to generate a high concentration of reactive species in a plasma chamber. [17] At the time of writing, few previous studies have reported the use of low-frequency (40 kHz) plasmas for the treatment of polymer materials under low-pressure. However, low-frequency plasmas have a range of advantages when compared to more commonly applied 13.56 MHz (RF) or 2.45 GHz (MW) frequencies, making them a viable alternative. A major advantage is that low-frequencies can generate a higher ion density than the higher RF or MW frequencies, which increases the uniformity of the plasma treatments. Additionally, low-frequency plasma is the most inexpensive form of plasma generation, as it requires the lowest amount of energy to generate. [18]

Plasma activation, or "plasma surface functionalization" refers to the increase in surface energy following an attachment or formation of functional groups from interactions with the plasma gas utilized. [19] It was known that typically, in low-pressure plasma systems, this surface modification is accompanied by a physical increase in surface roughness (plasma etching), which involves degradation and mass loss of the surface layers of a material on the nanoscale. [20] This observable mass loss of polymer materials increases as a function of treatment time [21], and is caused by ion bombardment of the material surface by the reactive plasma species, leading to a physical sputtering process. This process breaks up the surface polymer chains into smaller fragments, with the volatile, low molecular weight species being removed by the vacuum system, hence "etching" the surface. [22] Depending on the plasma system configurations and parameters employed, the etching can either lead to a slight increase in surface roughness, or a more pronounced formation of nano-pores and trenches. [23] For many applications, it is important to avoid this destructive surface roughening during surface modification procedures so that the treated material is not damaged in any way, ensuring that there are no drastic changes to the surface morphology or in the specular component of reflection of the material (change in color). [24] However, there has been no report on the plasma activation of nylon 6 polymers with low-frequency plasma in which parameters are selected to evade the etching process. Oxygen gas plasmas are often used to activate polymer and textile materials, to increase the hydrophilicity and adhesive properties of surfaces in preparation for bonding, coating, painting and printing. [25] Oxygen plasma activation proceeds through free radical oxidative reactions that lead to the incorporation of functionalities including carbonyl and hydroxyl groups. [26] However, oxygen gas plasmas can also trigger the aforementioned undesired etching effect if the parameters are not carefully selected. At suitably short treatment times with low plasma powers, the triggering of this

etching process can be avoided [12], enabling more energy-efficient conditions to be developed for plasma activation processes.

A major disadvantage of plasma treatments of polymer materials using reactive gases (such as O_2, N_2 and air) is the deterioration of the treatment level/functionalisation level of the materials over time; this is known as the ageing phenomenon, or hydrophobic recovery. This effect can limit the practical applications of the plasma treatments that are used in the hydrophilization of polymers. [27] A number of theories have been postulated in explaining this phenomenon, including the thermodynamically driven reorientation of polar groups away from the surface and into the bulk material, through rotations of the polymer chains. This has the effect of reducing the surface from a high energy state to a lower energy state, and can be considered as a relaxation process.[28] Further explanations for the ageing phenomenon include the migration of low molecular weight, non-polar species from the bulk material to the surface of the polymer, airborne surface contamination, the desorption of low molecular weight oxidised materials into the atmosphere, or contamination due to improper storage conditions.[29] Contact angle measurements prove to be an effective technique in monitoring the hydrophobic recovery of polymers, due to the resulting changes in surface energy caused by the migration and rotations of polymer chains. Following plasma activation, surface contact angle measurements tend to increase with time following this ageing process, due to the decrease in surface energy of the substrate. [30]

Although there have been a large number of studies and reviews summarising investigations of different plasma gas treatments on various polymer and textile materials [3, 12, 31], the complexity of plasma-substrate interactions has prevented a validated theory that relates and predicts changes in surface properties to specific process variables from being obtained. [32] Furthermore, the variation in plasma systems and plasma generation across the literature means that the parameters

required to achieve different plasma effects often have to be determined empirically. [33] Through isolating the surface functionalization/activation plasma process through parameter control, it has been possible to quantify the effects of varying the plasma exposure time of nylon 6 substrates.

In this article, we report on a series of plasma-treatment conditions that were used to activate nylon 6 plastic surfaces using low-frequency (40 kHz) oxygen plasma, without altering the surface morphology or bulk material properties. Analyzing the chemical changes in surface functionalities can often be challenging, as due to a lack of sensitivity, conventional analyses that monitor bulk properties cannot detect the nanoscale changes of functionalities that are induced by plasma treatments. [34] For this reason, a combination of surface-sensitive material characterization and imaging techniques have been utilized, to provide insights into the uniformity and underpinning mechanisms of oxygen plasma surface activation. Additionally, the effect of treatment time on the extent of surface functionalization obtained on the nylon 6 polymer surfaces was explored.

2. EXPERIMENTAL SECTION

2.1. Materials

Nylon 6 plastic sheets (natural nylon 6, 1.00 mm thickness, 1.14 g cm^{-3} density, extruded) were purchased from Direct Plastics Ltd (UK). All solvents (acetone, toluene) used in this study were AR grade ≥99.5% and purchased from Sigma-Aldrich (UK). 2,2-Diphenyl-1-picrylhydrazyl 95% (DPPH) was purchased from Fisher Scientific Ltd (UK). A Branson 1510 ultrasonic cleaning bath (USA) was used for cleaning samples at 160 W prior to plasma treatment. Plasma treatments were performed using a commercially available Diener Zepto Low-Pressure Plasma Laboratory Unit, supplied by Diener electronic GmbH & Co KG (Germany). The system comprised a cylindrical borosilicate glass chamber of 1.7 L volume, two semi-arc electrodes assembled axis-symmetrically

on the outer wall of the chamber, two needle valves with mass flow controllers for controlling process gas flow, a pirani gauge for chamber pressure measurement, an analogue timer, and a Pfeiffer Duo 3 rotary-vane vacuum pump (Germany) with an exhaust outlet for the process gas. The system had a working frequency of 40 kHz and had an adjustable power ranging from 0-100 W. The low-frequency plasma was generated by a capacitively-coupled plasma (CCP) discharge.

2.2. Plasma Surface Treatment of Nylon 6

Nylon 6 plastic sheets of various dimensions were initially cleaned through ultrasonic cleaning with acetone prior to the plasma treatments, to remove any surface impurities, dusts or hydrocarbon contaminants. The samples were fully submerged in a beaker containing acetone that was then placed in an ultrasonic cleaning bath filled with deionised water, operating at a power of 160 W for 10 minutes. The samples were subsequently left to dry in air. The dry samples were then treated with a low-frequency (40 kHz), low-pressure plasma at a power of 10 W, for exposure times between 10-40 s. The samples were placed in the center of the 1.7 L plasma chamber and the oxygen gas flow rate was held constant at 100 cm^3 min^{-1} for all treatments, with the working pressure kept between 0.2-0.5 mbar. After treatments, the samples were exposed to air for 30 s before being stored under vacuum until analysis.

2.3. Surface Characterization

Contact angle measurements were performed using a PGX Goniometer. Static contact angles of the nylon 6 plastic sheets were measured by initially placing 4 µl sessile water droplets on the polymer surfaces and allowing the droplets to equilibrate for 20 s. The contact angles of the droplets were then measured on the surfaces using a built-in camera. Measurements were performed at different positions of each sample, using three separate samples to test the uniformity

of each set of experimental conditions. Average values for the contact angles were then obtained from these three measurements. 1×1 cm plasma treated nylon 6 samples were analyzed by XPS using a Thermo Fisher Kα spectrometer, using monochromatic Al Kα radiation (72 W) at pass energies of 150 eV for survey scans, and 40 eV for high resolution scans, with 1.0 eV and 0.1 eV step sizes respectively. The angle between the photoelectron emission direction and plane of the sample was kept constant at 45°, and an area of approximately 400 µm was scanned. The XPS utilized low energy electrons and argon ions to prevent charge build-up on the nylon surfaces. Deconvolution of the high resolution C 1s spectra obtained was carried out using the line fitting function on CasaXPS 2.3.19 software, with a Shirley-type background subtraction, and FWHM set to 1.5 eV for all spectral components. For each set of experimental conditions, one spot was analysed on three separate samples to test the reproducibility and uniformity of the plasma treatments. Samples (1×1 cm) were analyzed by SSIMS using a Hiden Compact SIMS, with a MAXIM-600P detector using a Hiden 6 mm triple quadrupole mass filter with pulse ion detection. The samples underwent Ar^+ primary ion bombardment with a 25 nA primary current rastered over a 180×180 µm area at a 41° angle of incidence from normal, with 5.5 KeV impact energy. Surface radical densities were determined through a radical scavenging method, utilizing the molecule DPPH. A calibration graph of DPPH solutions in toluene was initially prepared, enabling the extinction coefficient, ε to be calculated. 1×1 cm untreated and plasma treated nylon 6 samples were immersed in 10 mL solutions of DPPH (1.0×10^{-4} M) in degassed toluene. The DPPH solution was heated for 3 hours at 80°C. The samples were then cooled to room temperature, and their absorptions were measured with a Varian Cary 50 UV-vis spectrophotometer at 520 nm (the maximum absorbance for DPPH). [35] Details of the calculations involved in the determination of surface radical densities can be found in the Supplementary Material. Samples were imaged

using an FEI Nova 450 SEM. The instrument operated with an FEG source in standard secondary electron and backscattered electron modes, operating at 3 kV. All samples were sputter-coated with an ultra-thin iridium layer (2 nm) prior to analysis. AFM images were obtained using a Bruker Innova microscope (USA) with a Nanoscope ADCS controller. A monolithic silicon cantilever with a resonant frequency of 300 kHz and force constant of 40 N/m was utilized in tapping mode, and 1×1 μm images were obtained. In order to study the ageing properties of the nylon 6 samples following plasma treatment, the samples were exposed to air under ambient conditions for time periods ranging between 0-20 days. The samples were then stored under vacuum until being analysed using static contact angle measurements and XPS.

3. RESULTS AND DISCUSSION

3.1. The Effects of Plasma Activation on Wettability

The wettability of the untreated and plasma treated samples was assessed using static contact angle measurements. From the contact angle measurements displayed in Figure 1, it can be seen that increasing the treatment times with oxygen plasma led to a relatively linear decrease in contact angle, with the overall hydrophilicity and wettability of the nylon 6 plastic sheets increasing. Although the untreated nylon 6 can already be considered to be slightly hydrophilic (contact angle value of 63.2±1.2°), the longest plasma exposure times saw a significant further increase in hydrophilicity, reaching the lowest value of 38.4±1.4° after 40 seconds. Compared to the untreated nylon 6 samples, there were also gradual reductions in contact angle after 10 seconds, 20 seconds, and 30 seconds respectively. These measurements were rationalized from XPS and SIMS data (discussed later), that confirmed the ability of the oxygen plasma to attach a number of "active" hydrophilic groups within the polymeric structure; this increased the overall wettability of the

nylon 6 substrates. The contact angle measurements were not influenced by any changes in surface morphology or roughness, as confirmed by the SEM and AFM images. It is also worth noting that different drop positons were tested on each of the sample surfaces, and the contact angle values did not vary significantly. This suggested that the uniform gas flow that was utilized in the low-pressure plasma treatment method had evenly distributed the surface chemical modifications across all areas of the substrates, with a large degree of reproducibility in the treatments.

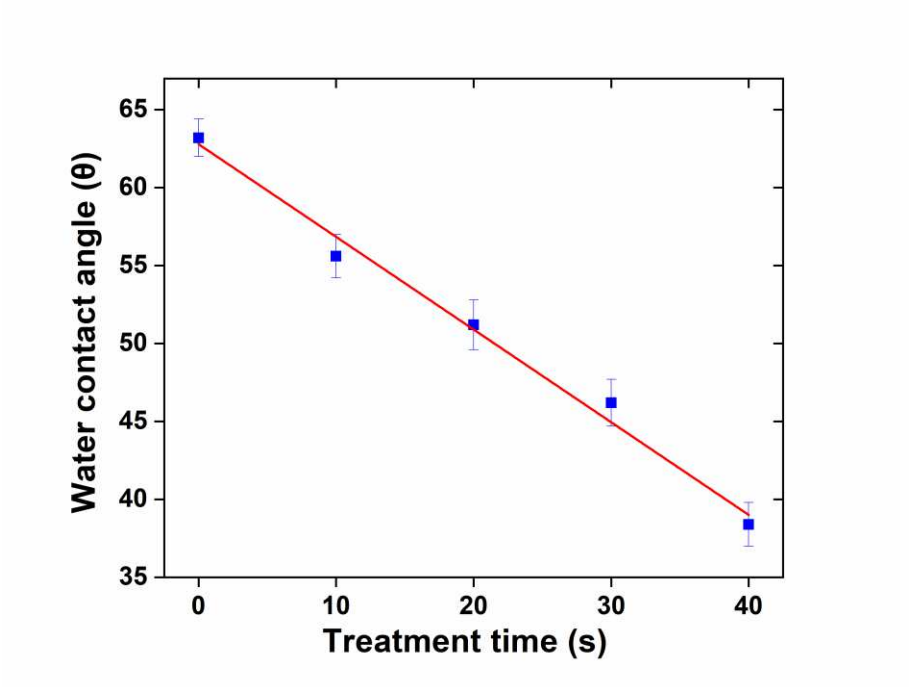

Figure 1. The variation in static water contact angle with plasma treatment time at 10 W.

3.2. The Effects of Plasma Activation on Surface Chemistry

The elemental composition data in Table 1 confirmed that with increasing plasma activation time, the percentage of carbon present on the nylon 6 surfaces deceased, whilst the oxygen content increased quite significantly. The nitrogen content remained at a similar level, suggesting that the

amide linkages within the nylon polymer chains were unaffected by the plasma exposure. There were also residual traces of silicon, calcium, sodium, and magnesium in each of the samples that were attributed to general surface contaminants; they were not reported in this study, due to their negligible amounts (<1%). After treatment for 10 s, the nylon 6 saw an increase in oxygen of 1.7% that suggested the ratio of oxygen-containing functional groups had increased within the polymer chains. The oxygen content then continued to increase progressively up to a maximum of 20.8% (increase of 8.5% compared to the untreated nylon 6) following 40 s of treatment. This was caused through the plasma-generated oxygen radical species reacting with the surface polymer chains of the nylon 6, forming reactive radical sites through hydrogen abstractions of the hydrocarbon backbones. These reactive radical centres then rearranged/recombined or reacted with oxygen upon exposure to air following the treatments, to produce more hydrophilic functionalities such as C-OH, C=O and O–C=O. From the errors shown in Table 1 (representing the standard deviations between the three samples under identical treatment conditions), it can be seen that the general variations for each elemental/functional group peak area were small, with the largest deviation being ± 2.6%. The small variations in the sample data suggested that the extent of the surface modifications induced by the plasma was relatively even at different positions in the plasma chamber, confirming that low-frequency, low-pressure plasma systems have the ability to produce uniform surface modifications to nylon 6 polymers within the plasma chamber.

Table 1. Elemental composition XPS data obtained for untreated and oxygen plasma treated nylon 6 samples.

Elemental composition (%)					C1s peak area (%)				
Treatment time (s)	**Carbon**	**Oxygen**	**Nitrogen**	**O/C ratio**	**C-C**	**C-N**	**C=O**	**C-O(H)**	**O-C=O**
0	76.0±1.1	12.3±0.3	10.0±0.4	0.16±0.01	69.0±0.4	16.3±0.2	14.7±0.4	0.0±0.0	0.0±0.0
10	75.0±1.3	14.0±1.0	10.3±0.4	0.19±0.02	62.8±0.9	16.4±0.2	15.8±0.6	4.1±0.3	0.9±0.2
20	70.5±1.1	17.7±0.9	10.1±0.2	0.25±0.02	59.9±2.6	16.2±0.9	16.4±1.5	5.9±0.3	1.6±0.6
30	69.0±1.1	18.5±1.3	10.1±0.5	0.27±0.02	59.2±1.3	15.9±0.4	15.8±0.7	7.0±0.4	2.1±0.6
40	66.8±1.4	20.8±0.7	10.2±0.7	0.31±0.02	58.5±1.9	15.6±0.3	15.4±1.6	7.2±0.7	3.3±0.3

Deconvolution of the C1s spectra of each of the samples has enabled the increase in surface oxygen content to be characterised further, showing the specific functional groups formed following oxygen plasma treatment. From the high resolution C1s XPS spectra shown in Figure 2 and the corresponding peak areas presented in Table 1, the changes in surface functionality following plasma activation are shown. These changes are also presented graphically in Figure 3a. In the untreated nylon 6 spectra displayed in Figure 2a, the functional groups identified as being present were C-C, C-N, and C=O. This corresponds to the functionalities present within the nylon 6 repeating unit, with the expected ratios for the nylon structure. Following plasma treatment for 10 s at 10 W, (Figure 2b) there was a slight increase in the percentage of C=O groups present when compared to the untreated samples (an increase of 1.1%). Also, newly formed C-OH (4.1%) and O-C=O (0.9%) functionalities were identified. They were attributed to the formation of hydroxyl groups and more heavily oxidised species in the form of carboxylic acid chain end groups. These groups were primarily formed through plasma oxidation and bond scission. As the treatment time

increased from 10-40 s, the at% of the newly incorporated C-OH and O-C=O groups also increased to maximum peak areas of 7.2% and 3.3% respectively, while the C-C concentrations decreased substantially.

The trends in Figure 3a clearly show that the largest increase in peak area with increasing treatment time was seen with the C-OH functional groups, with the O-C=O only seeing a slight increase over time. Having initially increased after 10 s of treatment, the C=O peak areas remained relatively constant between 20-40 s, with the C-N groups remaining relatively unchanged following all treatments. This indicated that the amide linkages within the nylon 6 repeat units were unaffected by the plasma activation process, with attachments of hydroxyl groups to the hydrocarbon backbones being the dominant mechanism of action in increasing the surface wettability of the substrates. From the O/C ratios shown in Figure 3b, a linear increase can be observed for the plasma treated nylon 6 samples with increasing activation time. Due to this increase in surface oxygen content, the increase in O/C ratio directly accounted for the linear decrease in measured contact angle values, and therefore increase in surface energy/hydrophilicity.

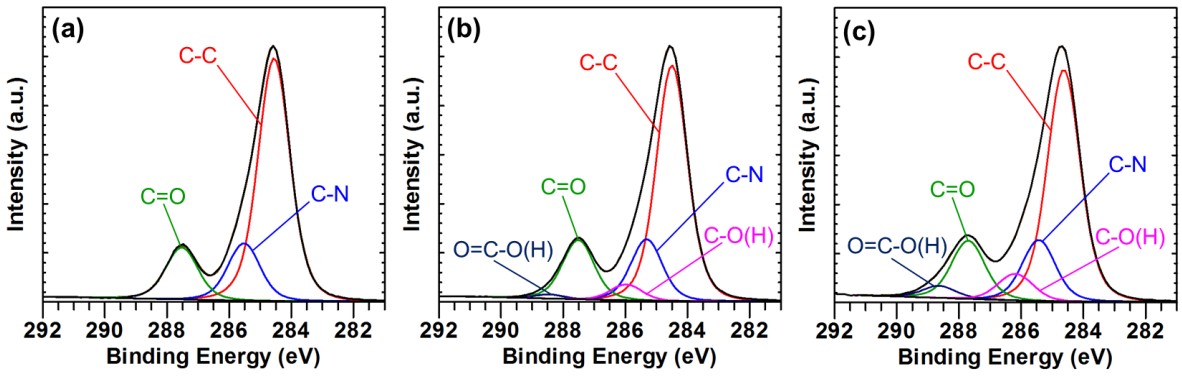

Figure 2. High resolution C1s XPS spectra with peak fittings of: (a) untreated nylon 6; (b) 10 s, 10 W oxygen plasma treated nylon 6 and (c) 40 s, 10 W oxygen plasma treated nylon 6.

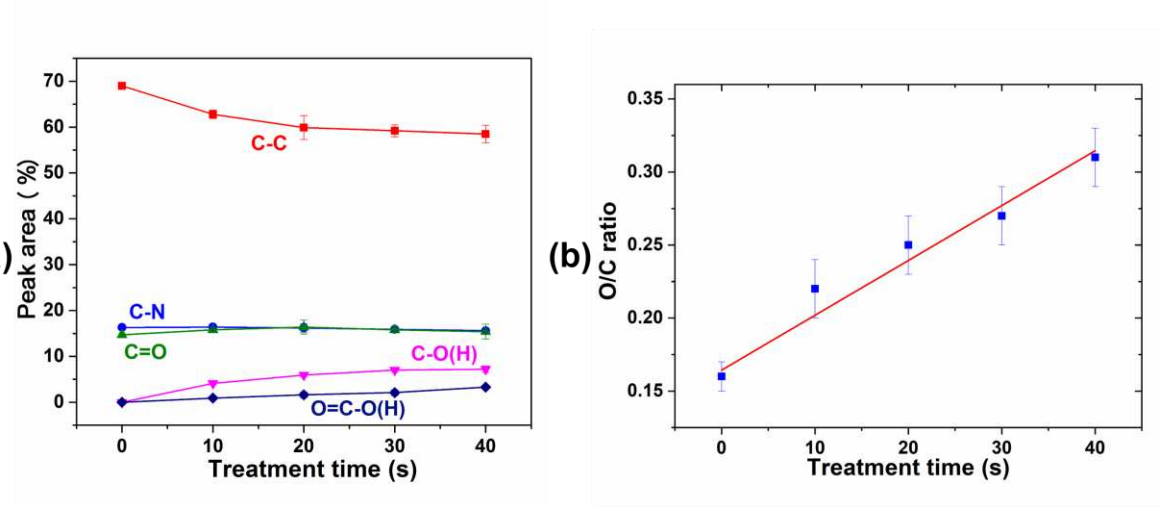

Figure 3. (a) The observed changes (%) in peak area for the different XPS peak fittings (b) O/C ratios of the plasma treated samples as a function of treatment time.

To complement the quantitative XPS data, SSIMS analysis was performed (Figure 4) to provide further details on the chemical species present on the nylon 6 surfaces following oxygen plasma exposure. From the untreated nylon 6 negative ion spectra shown in Figure 4a, the major peaks observed with the highest normalized intensities appeared at m/z = 1^- (H^-), 16^- (O^-) 26^- (C_2H^-), 42^- (CNO^-), 83^- ($C_5H_7O^-$), 112^- ($C_6H_{10}NO^-$, M^-H^-), 146^- ($C_7H_{12}NO_2^-$), and 199 ($C_{12}H_{25}NO^-$). The major assigned peaks in the positive ion spectra (Figure 4b) appeared at m/z = 1^+ (H^+), 16^+ (O^+), 28^+ (CO^+), 41^+ ($C_2H_3N^+$) and 55^+ ($C_3H_3O^+$) and 114 ($C_6H_{12}NO^+$, M^+H^+). All of these peaks can be considered to be expected fragments from the polyamide structure of the nylon 6 repeating unit, correlating to the functionalities present within the polymer. The peaks at m/z = 112 and 114 corresponded to the polymer repeating units as M^-H^- and M^+H^+ respectively.

The nylon 6 oxygen plasma treated negative ion spectrum for 40 s of plasma exposure at 10 W is displayed in Figure 4c. The major peaks observed were shown at m/z = 1^- (H^-), 16^- (O^-), 17^-

(OH^-), 25^- (C_2H^-), 26^- (CN^-), 36^- (C_3^-), 59^- ($C_2H_3O_2^-$), and 112^- ($C_6H_{10}NO^-$, M^-H^-). There were also a large number of new peaks with very low intensities that were present in the negative ion spectrum. The assigned peaks in the positive ion spectra (Figure 4d) appeared at m/z = 1^+ (H^+), 16^+ (O^+), 17^+ (OH^+), 28^+ (CO^+), 36^+ (C_3^+), 41^+ ($C_2H_3N^+$), 55^+ ($C_3H_3O^+$), 60^+ ($C_2H_4O_2^+$), and 114^+ ($C_6H_{12}NO^+$, M^+H^+). Similarly to the negative ion spectrum, a large number of new fragments with low relative intensities were also observed. Interestingly, in both the negative and positive ion spectra, the intensity of the oxygen peak at m/z = 16 increased following plasma exposure for 40 s. This aids in rationalizing the increase in O/C ratio observed in the XPS spectra, and the increase in wettability. It also confirms that the oxygen plasma incorporated polar oxygen-containing functionalities into the surface structure of the nylon 6 polymer. Additionally, the peak at m/z = 17 that was observed in both the positive and negative ion spectra with high intensities confirmed the presence of hydroxyl groups that had been incorporated into the nylon structures from exposure to the oxygen plasma species. The m/z = 112^- (M^-H^-) and 114^+ (M^+H^+) peaks in the negative and positive ion spectra respectively were both still present in the plasma treated samples, but their intensities had been vastly reduced. Although peaks with these intensities would not normally be assigned as significant peaks, they provided evidence that a small portion of the original nylon 6 surface structure were still present in the samples following plasma exposure. This suggested that under these low powered and short timescale treatments, the plasma action was not substantial enough to completely eradicate the original surface structure, with a small number of the nylon 6 chains still remaining intact. The peaks at m/z = 59^- ($C_2H_3O_2^-$), and 60^+ ($C_2H_4O_2^+$) were attributed to the formation of carboxylic acid groups in their deprotonated and protonated forms respectively. These polar groups were formed as chain end groups on the polymer chains following plasma induced chain scission and surface oxidation, and confirmed that the formed O-C=O bonds shown

in the XPS data can be attributed to carboxylic acid groups. It was evident from both the positive and negative ion spectra of the 40 s plasma treated surfaces that there were no intense peaks with m/z values > 100. However, the large number of newly formed, low intensity peaks with m/z > 100 was indicative of chain scission of the polymer chains, disrupting the long-range order in the polymer structures and increasing the extent of fragmentation. The large number of new peaks with low intensity also suggested that the chain scissions induced by the plasma treatments were not selective, and created a large number of new species with different chain lengths.

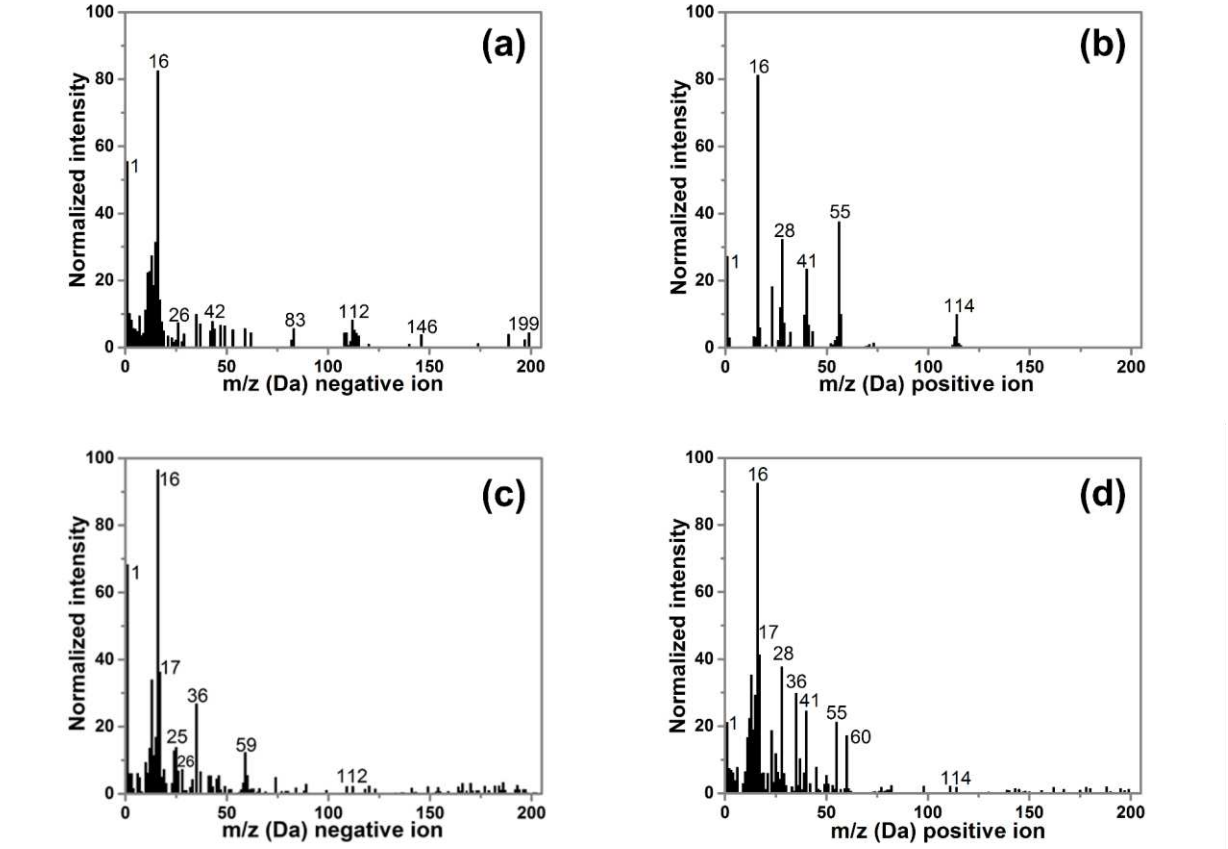

Figure 4. (a) SSIMS negative ion spectrum and (b) positive ion spectrum for untreated nylon 6. (c) SSIMS negative ion spectrum and (b) positive ion spectrum for oxygen plasma treated nylon 6 for 40 s at 10 W.

The surface densities of free radicals, including post-oxidation products such as peroxy radicals formed after exposure of the plasma activated samples to air were quantified using a radical scavenging method, which utilized the molecule DPPH. The extinction coefficient for DPPH in toluene was measured to be 11057 L mol^{-1} cm^{-1}, which is similar to values previously reported in the literature. [36] From the calculated values of free radical surface density shown in Figure 5, there was a general trend of increasing radical density with increasing plasma treatment time. There were some initial surface radicals detected in the untreated nylon 6 samples, which could be attributed to the DPPH undergoing undesired side reactions with the aliphatic chains in the nylon structure. Between the 10 and 40 s plasma treated samples, the radical surface densities were all in the range of 7.0-11.0×10^{-9} mol cm^{-2}. These values were of a similar order to that of previously reported radical densities for plasma treated polymer materials. [35, 37] The presence of radicals on the surface confirmed that plasma activation led to the formation of reactive radical sites, through hydrogen abstractions of the nylon 6 hydrocarbon backbone from oxygen radical species in the plasma. This aided in explaining the incorporation of oxygen containing hydroxyl and carbonyl groups, due to reactions of oxygen plasma species with these radical sites. In addition, the presence of surface radicals also accounts for the structural rearrangements that occur following chain scission, forming carboxylic acid chain end groups (detected in XPS and SSIMS analysis). The error bars were particularly large for each of the treated samples, which can be attributed to a variety of potential interfering factors in the DPPH radical scavenging method, such as the swelling effects of the toluene solvent on the nylon polymer surface, and potential side reactions that can occur between the highly reactive DPPH and some of the aliphatic chains within the polymer structure. Although this method of detecting and quantifying surface radicals has several limitations, such as the radical scavenger DPPH not having the ability to distinguish

between specific radical species, and the aforementioned interfering chemical species, it is still useful in providing mechanistic insights into the complex surface modification induced by plasma activation. The method is effective in complementing the XPS and SIMS data, providing information about the scale of the radical surface density following plasma activation, and showing the general trend of increasing radical density with increasing treatment time.

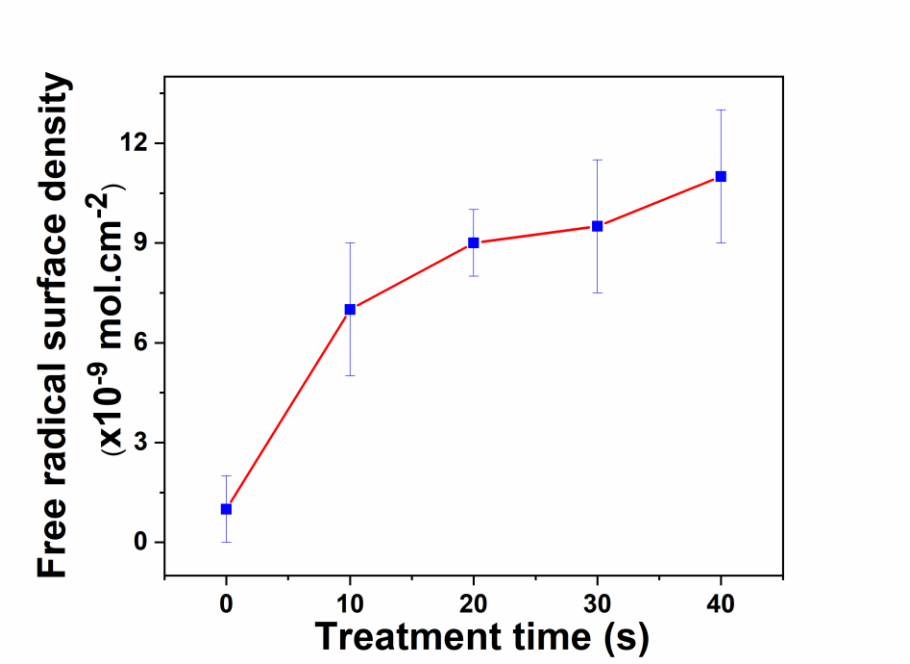

Figure 5. The free radical surface densities of untreated and oxygen plasma treated nylon 6 samples between 10-40 s at 10 W.

3.3. Surface Morphology and Roughness

The SEM images in Figure 6 show the surface morphology of the nylon 6 sheets both before and after low power (10 W) oxygen plasma exposure. The images confirm that there were no significant physical changes to the polymer surface morphology following exposure (40 s) to the

plasma at 10 W. Figure 6a shows that the untreated nylon 6 sheets were generally smooth with occasional grooves and a number of embedded surface particles. The EDX spectra of these particles were analysed and shown to have near-identical spectra to the smooth areas of the surface (see Supplementary Material). They were attributed to surface agglomerates formed from the manufacturing and processing of the nylon sheets. After oxygen plasma treatment for 40 seconds (Figure 6b), the surface of the polymer sheets and embedded particles did not change. Following longer treatment times, there were obvious changes to the surface morphology, with a significant increase in surface roughness due to plasma etching (see Supplementary Material for examples). This confirmed that under the selected conditions in this study, the conditions were non-destructive to the outer surface layers of the substrate, and the increase in hydrophilicity shown in the contact angle measurements (Figure 1) was caused entirely by a chemical change.

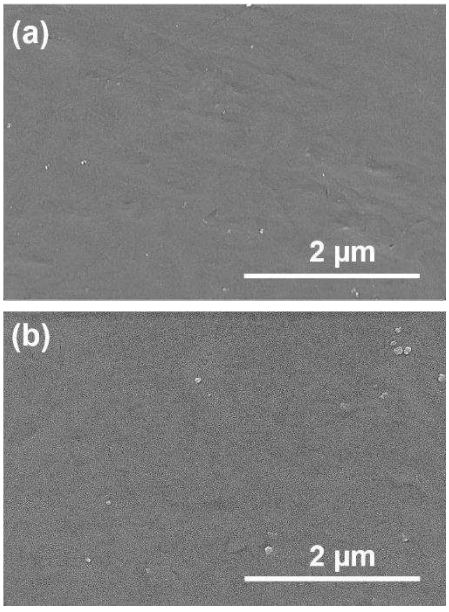

Figure 6. SEM images of (a) untreated nylon 6 and (b) oxygen plasma treated nylon 6 for 40 s at 10 W.

AFM was used to provide further details regarding the quantification of surface roughness of the samples before and after plasma activation. It is a well-known phenomenon that low-pressure plasma treatments of polymer materials generally have the effect of increasing the surface roughness. [38] However, under the conditions proposed in this study, the SEM images showed no obvious changes in surface morphology. The AFM images and corresponding surface roughness measurements shown in Figure 7 were in agreement with the SEM images, and confirmed that there had been no induced surface roughness in the plasma activated samples. The root mean square roughness (Rq) values for the untreated (7.47 nm) and 40 s oxygen plasma treated (6.96 nm) were both very similar, showing that the plasma had not increased the surface roughness. Although the roughness Rq value was slightly lower for the plasma treated surface, this difference was attributed to the general variation between different areas of the manufactured sheets that were present in all samples. The roughness average (Ra) values for the untreated (6.07 nm) and 40 s plasma treated (5.64 nm) were also both very similar, further confirming the lack of morphological change induced by the plasma. Both samples showed generally smooth surfaces, with a small areas of mild roughness. The highest points on the AFM images were attributed to the embedded surface particles, which had heights varying between 40-50 nm. The AFM data further confirmed that the plasma activation process that occurred under the selected conditions was an entirely surface chemical driven process, with no observed physical change in the nano-surface roughness or appearance.

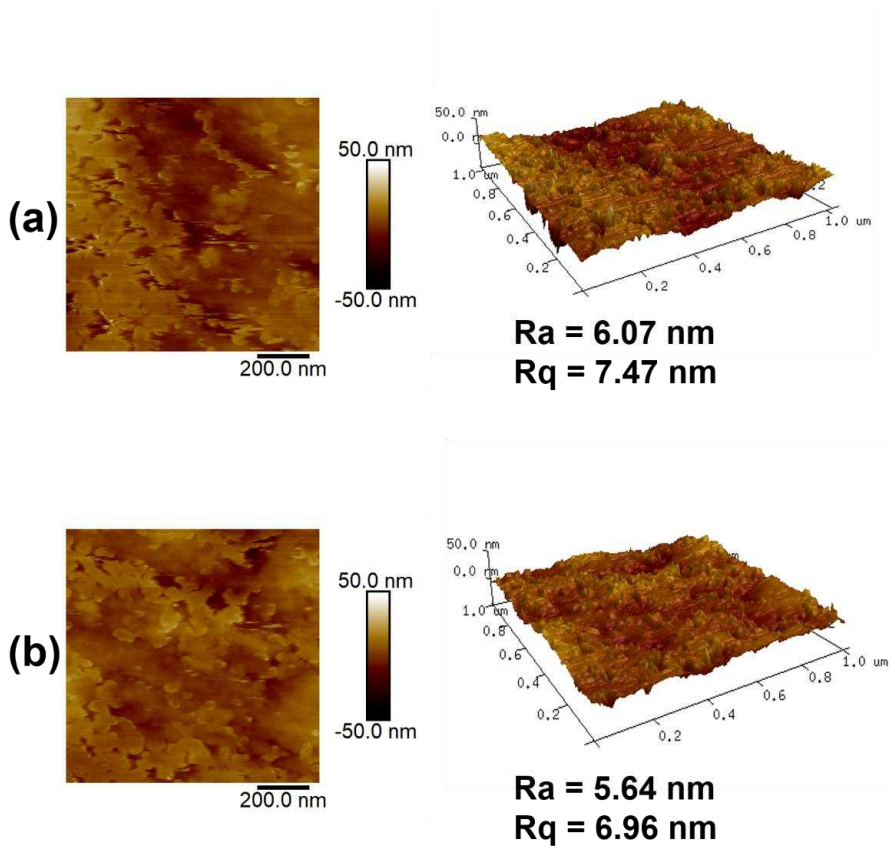

Figure 7. AFM images of: (a) untreated nylon 6; (b) oxygen plasma treated nylon 6 for 40 s at 10 W.

3.4. Ageing of samples post-plasma treatment

The graph in Figure 8a shows the observed decrease in surface wettability in the oxygen plasma activated nylon 6 samples, with subsequent ageing in air for 20 days. The samples initially saw a sharp increase in hydrophobic recovery, particularly following 1-5 days of ageing. This increase in hydrophobicity then started to become more gradual and levelled off after approximately 14 days, with prolonged exposure to air. The samples that had undergone shorter treatment times (10-20 s) showed a slower initial hydrophobic recovery than the longer treatments (30-40 s), but

the final contact values obtained were much higher for the shorter treatment times, indicating a higher degree of hydrophobicity. However, the samples treated for 40 s, had an overall increase in contact angle of 19.8° over the 20 day period, while the samples treated for 10 s only increased by 6.5°, indicating that larger degrees of plasma-surface functionalisation resulted in larger increases in the extent of hydrophobic recovery. This hydrophobic recovery was attributed to the reorientation of attached polar surface functionalities through the diffusion of oxidised low molecular weight species into the bulk material, and rotations of polar moieties away from the surface. This is a thermodynamically driven process that shifted the surface energy from a high energy (polar) state to a lower energy, and more stable state. [27] It was clear that none of the plasma activated nylon samples had fully reverted back to their initial surface wettability, suggesting that some of the attached polar functionalities present on the modified surfaces had remained. This is likely to have been due to some of the attached polar groups having intermolecular interactions with the water molecules in the air, which kept the groups at the surface.

XPS analysis was used to rationalize the trends in hydrophobic recovery seen in the contact angle measurements. Figure 8b shows O/C ratios for the aged nylon 6 samples that were initially treated with plasma for 40 s at 10 W. The initial reduction in O/C ratio was slight after 1 day of ageing, from 0.31 to 0.29. This decrease was much greater after 7 days to 0.19, at which point the O/C ratio levelled off, which appeared to follow the trend of increasing hydrophobic recovery seen through the contact angle measurements. It was clear that the polar groups had been released from the surface, through the thermodynamically favourable reorientation of the high energy polar groups away from the surface. The oxygen content did not drop to its initial untreated at% following 20 days of ageing for the activated sample, which can be attributed to the small amount

of moisture present in air, which could have interacted with some of the polar groups through hydrogen bonding, preventing them from reorienting away from the surface, hence keeping interfacial energy higher than the unmodified surface.

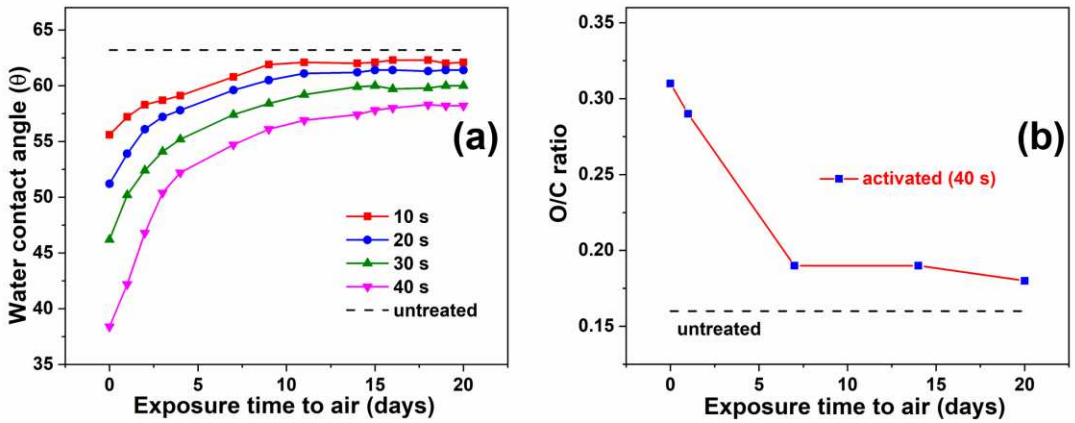

Figure 8. Graphs showing (a) static contact angle measurements and (b) O/C ratios (determined through XPS) of nylon 6 samples with increasing exposure time to air following plasma activation.

4. CONCLUSIONS

Through studying the effects of low-frequency, low-pressure oxygen plasma treatments on nylon 6 plastic sheets, mechanistic understandings of plasma activation in terms of physical properties, surface-chemistry, and morphology/roughness have been formed which can then be applied for use in the material processing and manufacturing industries for both plastics and textiles. The ageing of the activated samples following exposure to air has also been investigated. It has been found that activation increased the hydrophilicity of the nylon 6 surfaces, with increasing treatment time also enhancing this increase. XPS, SSIMS, and radical scavenging methods were used to

rationalize this increase in wettability in terms of surface chemistry, revealing, for the first time, that due to the combination of: 1) oxygen plasma increasing the number of attached polar functional groups (C-OH, C=O, COOH,); 2) the plasma increasing the fragmentation of nylon 6 polymer chains through oxidation and chain scission; 3) the plasma increasing the surface radical density with increasing treatment time, the hydrophilicity of the substrates increased. SEM and AFM imaging were then used to confirm that under the selected conditions for this study, there were no changes to the surface morphology or roughness, unlike many previously reported studies on low-pressure plasma treatments. Potential applications for the process include being used as prerequisite for applying coatings/paints to enhance coating adhesion, or as a general method for increasing the wettability of materials for bonding or printing, without inducing surface degradation or alterations in morphology.

ACKNOWLEDGMENT

The authors would like to thank the University of Leeds for providing the funding. XPS data collection was performed at the EPSRC National Facility for XPS ("HarwellXPS"), operated by Cardiff University and UCL.

REFERENCES

[1] U. Cvelbar, J.L. Walsh, M. Černák, H.W. de Vries, S. Reuter, T. Belmonte, C. Corbella, C. Miron, N. Hojnik, A. Jurov, H. Puliyalil, M. Gorjanc, S. Portal, R. Laurita, V. Colombo, J. Schäfer, A. Nikiforov, M. Modic, O. Kylian, M. Polak, C. Labay, J.M. Canal, C. Canal, M. Gherardi, K. Bazaka, P. Sonar, K.K. Ostrikov, D. Cameron, S. Thomas, K.-D. Weltmann, White paper on the

future of plasma science and technology in plastics and textiles, Plasma Process. Polym., 16 (2019) 1700228.

[2] L. Yu, G.Y. Chen, H. Xu, X. Liu, Substrate-Independent, Transparent Oil-Repellent Coatings with Self-Healing and Persistent Easy-Sliding Oil Repellency, ACS Nano, 10 (2016) 1076-1085.

[3] A. Zille, F.R. Oliveira, A.P. Souto, Plasma Treatment in Textile Industry, Plasma Process. Polym., 12 (2015) 98-131.

[4] N.W.M. Edward, P. Goswami, Plasma-based treatments of textiles for water repellency, in: J. Williams (Ed.) Waterproof and Water Repellent Textiles and Clothing, Woodhead Publishing, 2018, pp. 215-232.

[5] N.K. Vu, A. Zille, F.R. Oliveira, N. Carneiro, A.P. Souto, Effect of Particle Size on Silver Nanoparticle Deposition onto Dielectric Barrier Discharge (DBD) Plasma Functionalized Polyamide Fabric, Plasma Processes and Polymers, 10 (2013) 285-296.

[6] M. Jimenez, N. Lesaffre, S. Bellayer, R. Dupretz, M. Vandenbossche, S. Duquesne, S. Bourbigot, Novel flame retardant flexible polyurethane foam: plasma induced graft-polymerization of phosphonates, RSC Advances, 5 (2015) 63853-63865.

[7] P. Nguyen-Tri, F. Altiparmak, N. Nguyen, L. Tuduri, C.M. Ouellet-Plamondon, R.E. Prud'homme, Robust Superhydrophobic Cotton Fibers Prepared by Simple Dip-Coating Approach Using Chemical and Plasma-Etching Pretreatments, ACS Omega, 4 (2019) 7829-7837.

[8] C. Ma, L. Wang, A. Nikiforov, Y. Onyshchenko, P. Cools, K. Ostrikov, N. De Geyter, R. Morent, Atmospheric-pressure plasma assisted engineering of polymer surfaces: From high hydrophobicity to superhydrophilicity, Applied Surface Science, 535 (2021) 147032.

[9] M. Zhang, J. Pang, W. Bao, W. Zhang, H. Gao, C. Wang, J. Shi, J. Li, Antimicrobial cotton textiles with robust superhydrophobicity via plasma for oily water separation, Applied Surface Science, 419 (2017) 16-23.

[10] C. Wang, F. Hu, K. Yang, T. Hu, W. Wang, R. Deng, Q. Jiang, H. Zhang, Preparation and properties of nylon 6/sulfonated graphene composites by an in situ polymerization process, RSC Advances, 6 (2016) 45014-45022.

[11] Y. Guo, Y. Li, S. Wang, Z.-X. Liu, B. Cai, P.-C. Wang, Effect of silane treatment on adhesion of adhesive-bonded carbon fiber reinforced nylon 6 composite, International Journal of Adhesion and Adhesives, 91 (2019) 102-115.

[12] R.A. Jelil, A review of low-temperature plasma treatment of textile materials, Journal of Materials Science, 50 (2015) 5913-5943.

[13] T. Felix, J.S. Trigueiro, N. Bundaleski, O.M.N.D. Teodoro, S. Sério, N.A. Debacher, Functionalization of polymer surfaces by medium frequency non-thermal plasma, Applied Surface Science, 428 (2018) 730-738.

[14] E. Kraus, L. Orf, B. Baudrit, P. Heidemeyer, M. Bastian, R. Bonenberger, I. Starostina, O. Stoyanov, Analysis of the low-pressure plasma pretreated polymer surface in terms of acid–base approach, Applied Surface Science, 371 (2016) 365-375.

[15] D. Štular, G. Primc, M. Mozetič, I. Jerman, M. Mihelčič, F. Ruiz-Zepeda, B. Tomšič, B. Simončič, M. Gorjanc, Influence of non-thermal plasma treatement on the adsorption of a stimuli-responsive nanogel onto polyethylene terephthalate fabric, Progress in Organic Coatings, 120 (2018) 198-207.

[16] M.Y. Naz, S. Shukrullah, Y. Khan, A. Ghaffar, N.U. Rehman, S. Ullah, Actinometry study on dissociation fraction in low pressure capactively coupled Ar–O2 mixture plasma, High Energy Chemistry, 49 (2015) 449-458.

[17] L. Bárdos, H. Baránková, Plasma processes at atmospheric and low pressures, Vacuum, 83 (2008) 522-527.

[18] Y. Chen, D. Shi, Y. Chen, X. Chen, J. Gao, N. Zhao, C.-P. Wong, A Facile, Low-Cost Plasma Etching Method for Achieving Size Controlled Non-Close-Packed Monolayer Arrays of Polystyrene Nano-Spheres, Nanomaterials (Basel), 9 (2019) 605.

[19] S. Kaya, P. Rajan, H. Dasari, D.C. Ingram, W. Jadwisienczak, F. Rahman, A Systematic Study of Plasma Activation of Silicon Surfaces for Self Assembly, ACS Applied Materials & Interfaces, 7 (2015) 25024-25031.

[20] P. Zhao, N. Qin, C.L. Ren, J.Z. Wen, Surface modification of polyamide meshes and nonwoven fabrics by plasma etching and a PDA/cellulose coating for oil/water separation, Applied Surface Science, 481 (2019) 883-891.

[21] H. Puliyalil, U. Cvelbar, Selective Plasma Etching of Polymeric Substrates for Advanced Applications, Nanomaterials, 6 (2016) 108.

[22] R. Morent, N. De Geyter, J. Verschuren, K. De Clerck, P. Kiekens, C. Leys, Non-thermal plasma treatment of textiles, Surface and Coatings Technology, 202 (2008) 3427-3449.

[23] I. Junkar, U. Cvelbar, A. Vesel, N. Hauptman, M. Mozetič, The Role of Crystallinity on Polymer Interaction with Oxygen Plasma, Plasma Process. Polym., 6 (2009) 667-675.

[24] H.-R. Lee, D.-j. Kim, K.-H. Lee, Anti-reflective coating for the deep coloring of PET fabrics using an atmospheric pressure plasma technique, Surface and Coatings Technology, 142-144 (2001) 468-473.

[25] A. Vesel, M. Mozetic, New developments in surface functionalization of polymers using controlled plasma treatments, Journal of Physics D: Applied Physics, 50 (2017) 293001.

[26] K. Tsougeni, N. Vourdas, A. Tserepi, E. Gogolides, C. Cardinaud, Mechanisms of Oxygen Plasma Nanotexturing of Organic Polymer Surfaces: From Stable Super Hydrophilic to Super Hydrophobic Surfaces, Langmuir, 25 (2009) 11748-11759.

[27] M. Mortazavi, M. Nosonovsky, A model for diffusion-driven hydrophobic recovery in plasma treated polymers, Applied Surface Science, 258 (2012) 6876–6883.

[28] D. Hegemann, E. Lorusso, M.-I. Butron-Garcia, N.E. Blanchard, P. Rupper, P. Favia, M. Heuberger, M. Vandenbossche, Suppression of Hydrophobic Recovery by Plasma Polymer Films with Vertical Chemical Gradients, Langmuir, 32 (2016) 651-654.

[29] E. Bormashenko, G. Chaniel, R. Grynyov, Towards understanding hydrophobic recovery of plasma treated polymers: Storing in high polarity liquids suppresses hydrophobic recovery, Applied Surface Science, 273 (2013) 549-553.

[30] A. Vesel, I. Junkar, U. Cvelbar, J. Kovac, M. Mozetic, Surface modification of polyester by oxygen- and nitrogen-plasma treatment, Surface and Interface Analysis, 40 (2008) 1444-1453.

[31] Y. Kusano, Atmospheric Pressure Plasma Processing for Polymer Adhesion: A Review, The Journal of Adhesion, 90 (2014) 755-777.

[32] E. Bormashenko, G. Whyman, V. Multanen, E. Shulzinger, G. Chaniel, Physical mechanisms of interaction of cold plasma with polymer surfaces, Journal of Colloid and Interface Science, 448 (2015) 175-179.

[33] F. Khelifa, S. Ershov, Y. Habibi, R. Snyders, P. Dubois, Free-Radical-Induced Grafting from Plasma Polymer Surfaces, Chemical Reviews, 116 (2016) 3975-4005.

[34] L.A. Can-Herrera, A. Ávila-Ortega, S. de la Rosa-García, A.I. Oliva, J.V. Cauich-Rodríguez, J.M. Cervantes-Uc, Surface modification of electrospun polycaprolactone microfibers by air plasma treatment: Effect of plasma power and treatment time, European Polymer Journal, 84 (2016) 502-513.

[35] D. O. H. Teare, W. Schofield, R. P Garrod, J. P. Badyal, Rapid Polymer Brush Growth by TEMPO-Mediated Controlled Free-Radical Polymerization from Swollen Plasma Deposited Poly(maleic anhydride) Initiator Surfaces, Langmuir : the ACS journal of surfaces and colloids, 21 (2005) 10818-10824.

[36] S.B. Kedare, R.P. Singh, Genesis and development of DPPH method of antioxidant assay, J Food Sci Technol, 48 (2011) 412-422.

[37] R. Teng, H.Yasuda, Polymers, Ex Situ Chemical Determination of Free Radicals and Peroxides on Plasma Treated Surfaces, Plasmas and Polymers, 7 (2002) 57-69.

[38] D. Hetemi, J. Pinson, Surface functionalisation of polymers, Chemical Society Reviews, 46 (2017) 5701-5713.

Supplementary Material

Low-Frequency Plasma Activation of Nylon 6

Richard Thompson[a], David Austin[b], Chun Wang[c], Anne Neville[c], and Long Lin,[a]*

[a]Department of Color Science, School of Chemistry, University of Leeds, Leeds, LS2 9JT, U.K.

[b]School of Chemical and Process Engineering, University of Leeds, Leeds, LS2 9JT, U.K.

[c]Institute of Functional Surfaces, School of Mechanical Engineering, University of Leeds, Leeds, LS2 9JT, U.K.

FT-IR Spectroscopy. FT-IR spectroscopy was used in attempts to detect changes in the surface functionalities of the nylon 6 substrates following plasma activation. FT-IR measurements of the nylon 6 samples were obtained using a PerkinElmer Spectrum One Spectrometer in reflectance mode, with the scanning range between 500 and 4000 cm^{-1}. From the FT-IR spectra shown in Figure S1, it is evident that there were no obvious changes in the spectra of the untreated or plasma activated samples under different conditions. This can be attributed to the lack of sensitivity of the technique towards the nano-scale surface modifications. For this reason, XPS and SSIMS analysis were used to characterize the surfaces in this study.

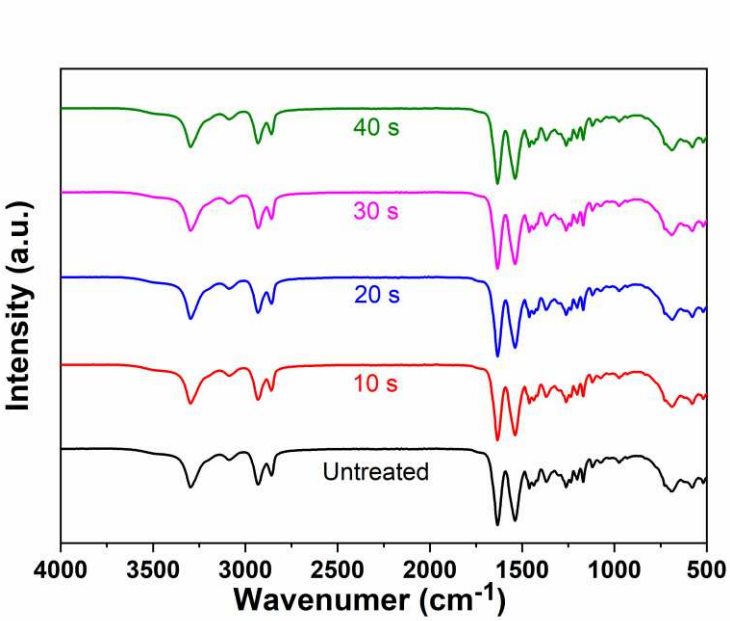

Figure S1. FT-IR spectra of untreated and plasma treated nylon 6 samples at 10 W for different treatment times.

Determination of Surface Radical Densities. As mentioned in the main article, a radical scavenging method was used to determine the surface radical densities of the plasma-activated nylon 6 sheets. The molecule DPPH was utilized in labelling the radical species, and a calibration graph of DPPH solutions in toluene was initially prepared. This calibration graph is shown in Figure S2 and using the graph, the extinction coefficient, ε was calculated to be 11057 L mol^{-1} cm^{-1}. To determine the surface radical densities of the untreated and plasma-activated nylon 6, 1×1 cm^2 samples were immersed in 10 ml solutions of DPPH (1.0×10^{-4} M) in degassed toluene. The DPPH solutions were heated for 3 hours at 80°C. The samples were then cooled to room temperature, and their absorptions were measured with a Varian Cary 50 UV-vis spectrophotometer at 520 nm (the maximum absorbance for DPPH). [1] The surface radical

densities of the untreated and plasma-treated samples were then calculated using Equations 1 and 2 respectively:

$$d_{Untreated} = \frac{[DPPH]_{Blank} - [DPPH]_{Treated}}{V \times S} \quad (1)$$

$$d_{Activated} = \frac{[DPPH]_{Untreated} - [DPPH]_{Treated}}{V \times S} \quad (2)$$

Where $d_{Untreated}$ = surface radical density of the untreated nylon 6, $d_{Activated}$ = surface radical density of the plasma activated nylon 6 substrates, $[DPPH]_{Blank}$ = concentration of DPPH remaining after heating the solution without the substrate, $[DPPH]_{Untreated}$ = concentration of DPPH remaining after heating with the untreated sample, $[DPPH]_{Treated}$ = concentration of DPPH remaining after heating with the treated substrate, V = volume of DPPH solution, and S = surface area of the substrate.

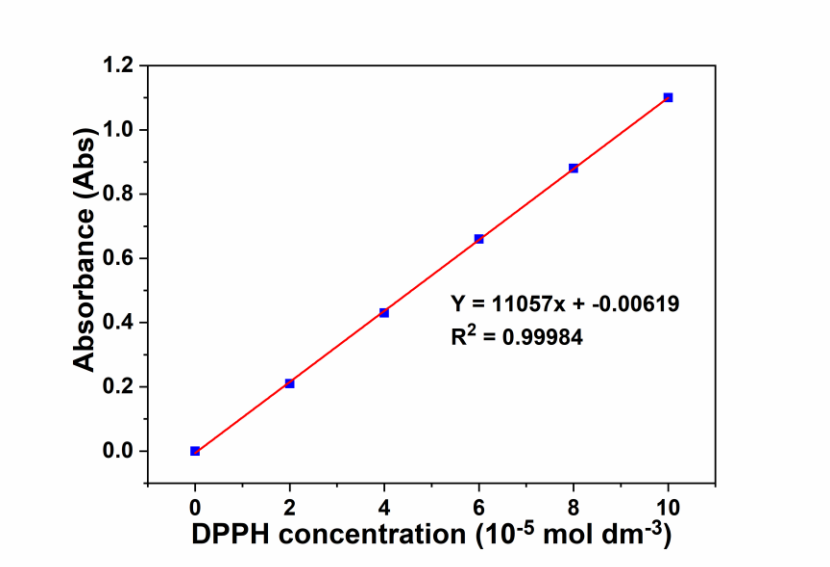

Figure S2. Calibration graph for DPPH in toluene. Absorbance measured at λ_{max} = 520 nm for DPPH.

Comparisons of Plasma Activation and Plasma Etching using SEM Imaging. To compare the effects of plasma activation with those of plasma etching, SEM images of untreated nylon 6 and samples treated with low-pressure plasma under different conditions are shown. Figures S3a and b show the untreated nylon 6 sample and activated sample (40 s, at 10 W) respectively. It confirms that there were no major changes to the surface morphology or roughness following plasma exposure under these conditions. Figure S3c shows a plasma etched nylon 6 surface, obtained from treating the sample with plasma for an extended period (600 s, at 10 W). The nylon surface has clear well-defined nano-grooves and cracks. This etching process is caused by a stochastic surface ion bombardment process, which occurs at longer treatment times and higher plasma powers than those utilized in this study on plasma activation (this study aimed to avoid this nano-scale degradation of the surfaces).

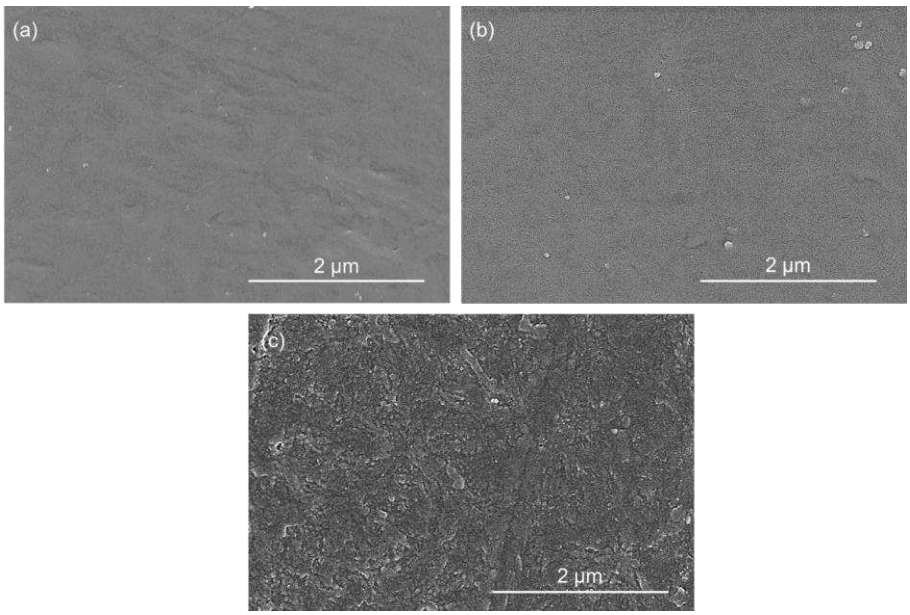

Figure S3. SEM images of (a) untreated nylon 6; (b) oxygen plasma treated nylon 6 for 40 s at 10 W; (c) oxygen plasma treated nylon 6 for 600 s at 10 W.

EDX analysis of surface agglomerates. To identify the surface nanoparticles observed in the untreated nylon 6 samples following solvent cleaning with acetone, EDX measurements were obtained using an EDAX (AMTEL) coupled with the FEI Nova 450 SEM instrument, utilizing TEAM EDS software for elemental analysis. As shown in Figure S4, the EDX spectra of the smooth areas of the cleaned nylon 6 surfaces and the areas containing a number of surface nanoparticles were almost identical. The major element detected was carbon, with some residual nitrogen, oxygen and iridium peaks (due to sputter-coating) also being presented. This confirmed that the surface particles were organic, and were attributed to surface agglomerates formed from the manufacturing and processing of the nylon 6 sheets.

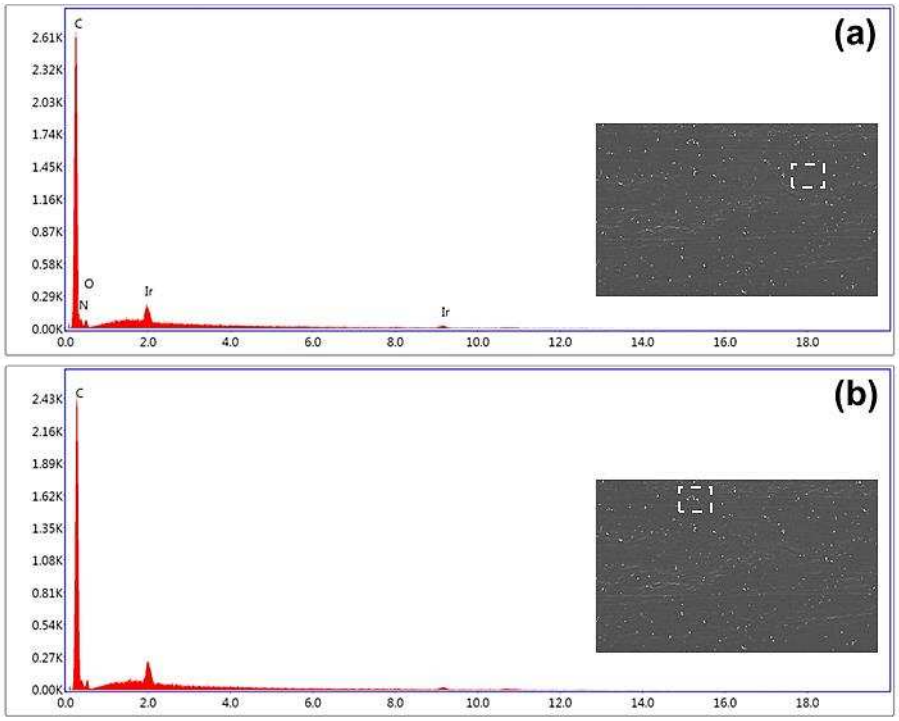

Figure S4. EDX spectra showing (a) the smoother areas of the nylon 6 surface and (b) the area of the nylon 6 surface containing surface nanoparticles/agglomerates with magnification 3500×.

Crystallinity. XRD measurements were obtained using a Bruker D8 diffractometer (USA). Copper Kα radiation (λ=1.0541 nm) was used to obtain spectra with 2θ values ranging between 5-90°, with steps of 0.05° and a rate of 0.2 s/step. The samples were not rotated upon exposure to the copper radiation. From the XRD data displayed in Figure S5, it is apparent that there were no changes in the crystallinity of the plasma treated nylon 6 samples. Under the selected conditions, oxygen plasma surface activation did not alter the degree of crystallinity or result in the formation of new crystalline species. The major 2θ peak shown in the XRD spectra for nylon 6 appeared as a broad peak at 24°, confirming the sheets to be mostly amorphous. There were no major shifts or changes in the spectra for the activated samples compared against the untreated samples. The crystallinities of all of the untreated and oxygen plasma treated samples ranged between 39.3-40.6 %. This range can be attributed to the associated error in the XRD, in addition to the expected slight variation in each of the manufactured nylon 6 plastic sheet samples. The results confirmed that there were no significant changes in crystallinity induced by plasma activation, and that the polymer chain arrangements in the nylon 6 sheets were predominantly amorphous, both before and after plasma exposure.

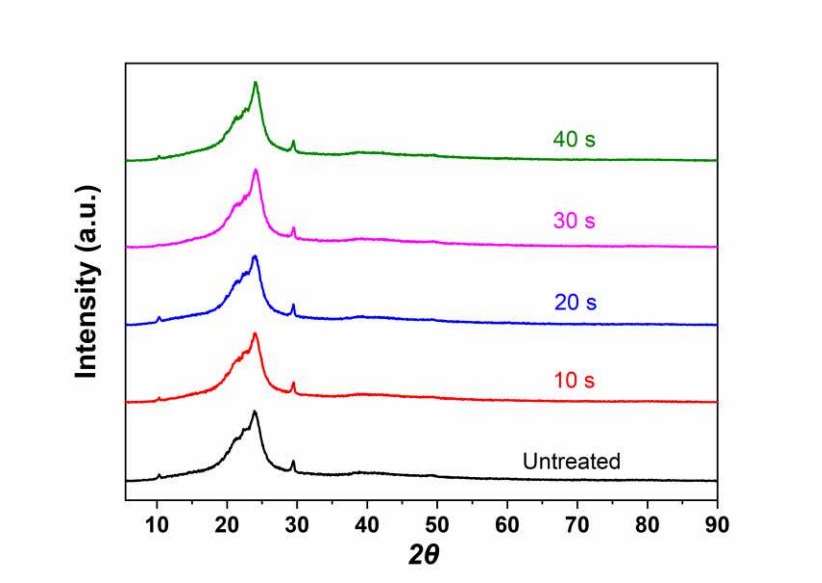

Figure S5. XRD spectra of the untreated and oxygen plasma treated nylon 6 samples between 10-40 s at 10 W.

To complement the XRD data, and give further insights into the effects of plasma activation on crystallinity, DSC analysis was carried out using a DSC Q20 model (TA Instruments, USA), with a heating rate of 10°C/min, increasing from 25 to 250°C under a nitrogen atmosphere. The nitrogen flow rate was 50 mL/min. The initial heating and controlled cooling were carried out to remove the thermal history from the samples. Values for crystallinity were derived using the literature enthalpy value of 230 J g^{-1} for 100 % nylon 6. [2] The thermal analysis data obtained from the DSC measurements are shown in Figure S6 and Table S1. From the obtained values for crystallinity, it can be seen that there were no major changes between the untreated nylon 6 and plasma-treated nylon 6 for 40 s. There was an increase in crystallinity of 1.66 %, which could either indicate that there was a slight increase in crystallinity following plasma activation that XRD was not sensitive enough to detect, or that the small measured change could be attributed to the associated errors in the DSC measurements, with the DSC supporting the XRD data in showing that plasma activation does not change the crystallinity of the nylon 6 sheets in a major way.

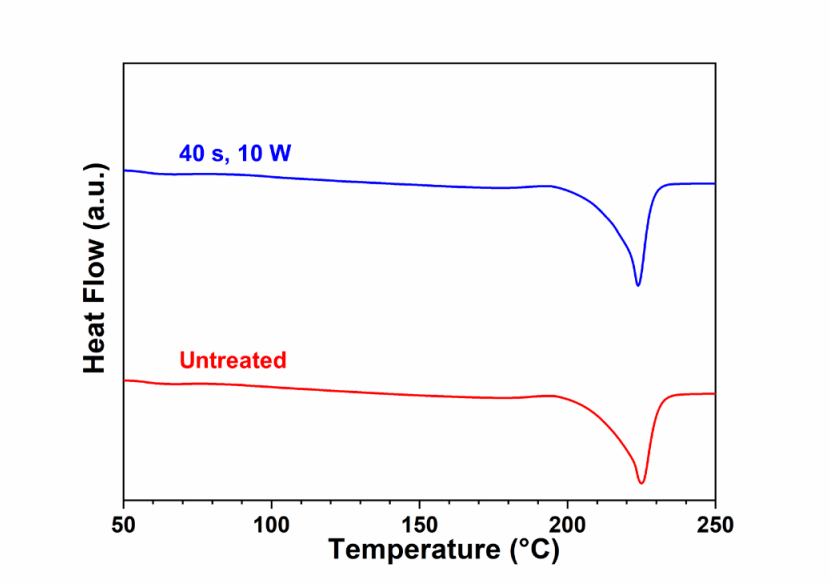

Figure S6. DSC curves of untreated nylon 6 and oxygen plasma treated nylon 6 for 40 s at 10 W.

Table S1. DSC thermal analysis data for untreated nylon 6 and plasma activated nylon 6.

Sample	Cycle number	Transition peak Temperature (°C)	Transition energy (Joules/gram)	Crystallinity (%)
Untreated nylon 6	1 / heat	225.03	82.33	-
Untreated nylon 6	2 / cool	192.88	72.60	-
Untreated nylon 6	3 / reheat	221.51	57.13	24.84
40 s, 10 W nylon 6	1 / heat	224.56	80.40	-
40 s, 10 W nylon 6	2 / cool	192.85	70.53	-
40 s, 10 W nylon 6	3 / reheat	221.67	60.96	26.50

REFERENCES (Supplementary Material)

[1] D. O. H. Teare, W. Schofield, R. P. Garrod, J. P. Badyal, Rapid Polymer Brush Growth by TEMPO-Mediated Controlled Free-Radical Polymerization from Swollen Plasma Deposited Poly(maleic anhydride) Initiator Surfaces, Langmuir : the ACS journal of surfaces and colloids, 21 (2005) 10818-10824.

[2] C. Millot, L.-A. Fillot, O. Lame, P. Sotta, R. Seguela, Calorimetry, Assessment of polyamide-6 crystallinity by DSC, 122 (2015) 307-314.